Macro Basis Function Framework for Solving Maxwell's Equations in Surface Integral Equation Form

Forum for Electromagnetic Research Methods and Application Technologies (FERMAT)

Macro Basis Function Framework for Solving Maxwell's equations in Surface-Integral-Equation Form

C. Craeye[(1)], J. Laviada[(2)], R. Maaskant[(3)], and R. Mittra[(4)]
[(1)]ICTEAM Institute, Université catholique de Louvain,
1348 Louvain-la-Neuve, Belgium
(e-mail: christophe.craeye@uclouvain.be)
[(2)]Área de Teoría de la Señal y Comunicaciones, Universidad de Oviedo
33203, Gijón (Asturias), Spain
(Email: jlaviada@tsc.uniovi.es)
[(3)]Dept. of Signals & Systems, Chalmers Univ. of Techn.,
Gothenburg, Sweden
(e-mail: rob.maaskant@chalmers.se)
[(4)]Electromagnetic Communication Laboratory, The Pennsylvania State University,
University Park, PA 16802, USA
(Email: rajmittra@ieee.org)

***Abstract*—The Macro Basis Functions (MBFs) approach is a form of domain-decomposition method applied to radiation and scattering problems solved by using integral-equation techniques. It enables a systematic reduction of the number of degrees of freedom, from that imposed by the discretization of the surfaces to that associated with the physical limits of field distributions. This paper reviews different variants of this approach, including the techniques for determining the MBFs and for fast calculation of their interactions. The link with Krylov-subspace iterative methods is described, the relationship between the surface of subdomains and the number of physical degrees of freedom is discussed and multi-level schemes are revisited. Finally, avenues for further research are outlined in the Conclusions section of this paper.**

***Index Terms*—macro basis functions, integral equations, method of moments, characteristic basis functions, synthetic functions**

I. Introduction

Efficient and accurate solution of electromagnetic-field integral equations has been an important research topic for many years. Despite the availability of computers with fast CPUs and abundant as well as affordable memory resources, ever-increasing demand for solving larger problems still outpaces the rapid advances in numerical techniques. The challenges faced almost a decade ago were described in a review paper [1] and the domain-decomposition approach was introduced around the same time frame to solve large problems by using the "divide and conquer" approach. One such methodology is based on expressing the solutions in the subdomains in terms of high-level basis functions that are linear combinations of a number of pre-computed solutions for the isolated subdomains, or for those domains surrounded by relatively small neighborhoods. Such a divide and conquer concept was already present in earlier works such as [2]–[4] and has been developed more systematically by Suter and Mosig [5], who introduced the expression "Macro Basis Function" (MBF). Quite a few other methods based on aggregation of low-level basis functions, such as [6], [7] appeared in the computational electromagnetics (CEM) literature almost contemporaneously, or soon thereafter. The main attribute of the domain decomposition approach is that it enables us to handle considerably larger problems, in terms of number of Degrees of Freedom (DoFs) than is possible by using the conventional Method of Moments (MoM).

Our objectives in this paper are to review some of the earlier works, present the latest developments in this area and provide new perspectives on this class of methods. In order to facilitate the understanding of the following sections, Section II briefly describes what may be viewed as an elementary MBF approach, while Section III provides a summary of associated methods. Section IV explains how MBFs can be generated, while Section V describes different techniques for fast calculation of interactions between the MBFs. Following this, Section VI reviews the link between MBF approaches and modern iterative techniques and Section VII addresses the important challenges encountered when attempting to solve multi-scale problems. Finally, Section VIII briefly summarizes this work and presents some perspectives on the future directions.

II. Elementary MBF approach

This section summarizes what may be regarded as the simplest possible MBF approach. For reasons that will be apparent later, it may not be the most effective numerical

approach, but it will be used to introduce the terminologies and notations, while laying the foundations of what is to follow. We will assume that the reader is already familiar with the Method of Moments (MoM).

Let us write the original MoM system of equations as $\mathbf{Z}\,\mathbf{x} = \mathbf{v}$ in which $\mathbf{Z}$ is the MoM impedance matrix, $\mathbf{x}$ is the column vector containing the expansion coefficients to be determined and $\mathbf{v}$ is the excitation vector, which corresponds to the tested incident fields. Next, we divide the computational subdomain into a number of contiguous sub-domains, and postulate that the solution on each subdomain can be found in the subpsace spanned by a number of precomputed subdomain solutions, referred to as the Macro Basis Functions and denoted by the column vector $\mathbf{q}_{ik}$, where i is the index of the subdomain and k in the index of an MBF defined on that subdomain. The above MBFs need to be carefully chosen, and how to do this will be discussed in detail in Section IV. For the sake of simplicity, we will assume that the indices of all basis functions in a given subdomain are consecutive. It is then easy to identify *blocks* of the MoM impedance matrix associated with testing and basis functions on specific pairs of subdomains. One can also identify *segments* of the excitation vector, residual, or solution vector; those segments describe tested fields or current distributions on specific subdomains. If $\mathbf{Q}_i$ denotes the matrix whose columns are comprised of the MBFs $\mathbf{q}_{ik}$, then, for the ith segment of $\mathbf{x}$, we assume that $\mathbf{x}_i = \mathbf{Q}_i\,\mathbf{y}_i$, for the i-th segment of $\mathbf{x}$. The reduction of unknowns arises from the fact that vector $\mathbf{y}_i$ contains much fewer unknowns than vector $\mathbf{x}_i$ (typically by one to two orders of magnitude). By applying Galerkin testing, i.e., by choosing the set of macro testing functions identical to the set of macro basis functions, we obtain [6]:

$$\begin{bmatrix} \mathbf{Q}_1^H\,\mathbf{Z}_{11}\,\mathbf{Q}_1 & \dots & \mathbf{Q}_1^H\,\mathbf{Z}_{1N}\,\mathbf{Q}_N \\ \vdots & \ddots & \vdots \\ \mathbf{Q}_N^H\,\mathbf{Z}_{N1}\,\mathbf{Q}_1 & \dots & \mathbf{Q}_N^H\,\mathbf{Z}_{NN}\,\mathbf{Q}_N \end{bmatrix} \begin{bmatrix} \mathbf{y}_1 \\ \vdots \\ \mathbf{y}_N \end{bmatrix} = \begin{bmatrix} \mathbf{Q}_1^H\mathbf{v}_1 \\ \vdots \\ \mathbf{Q}_N^H\mathbf{v}_N \end{bmatrix} \tag{1}$$

where $\mathbf{Q}^H$ denotes the transposed conjugate of $\mathbf{Q}$. In many implementations, just the transpose operation is applied, and it is difficult to say which one of these two options yields a better result. Since the matrices $\mathbf{Q}_i$ have much fewer columns than lines, a very strong compression of the original system of equations is achieved.

One should note that the original MBF approach [5] also employs elementary basis functions that "bridge" consecutive subdomains and that the real and imaginary parts of the MBFs are treated separately. These two refinements have either not been retained, or they have been integrated in different forms in subsequent MBF developments.

It is interesting to note that the i-th block-line of (1) can be written as:

$$\mathbf{Q}_i^H\ \left([\mathbf{Z}\,\mathbf{x}^{\text{MBF}}]_i - \mathbf{v}_i\right) = 0 \tag{2}$$

where $\mathbf{x}^{\text{MBF}}$ is the solution obtained by using MBFs, and $[\mathbf{g}]_i$ denotes the i-th segment of a vector $\mathbf{g}$ (in the following, the brackets will in general be omitted). The expression between parentheses is nothing else than the opposite of segment i of the residual ($\mathbf{r} = \mathbf{v} - \mathbf{Z}\,\mathbf{x}$). This means that, as a result of Galerkin testing, the MBFs defined on a given subdomain are orthogonal to the segment of the residual corresponding to the same subdomain.

III. Historical perspective

As mentioned in the introduction, MBF-type methods rely on a divide-and-conquer approach to solve, through an integral-equation formulation, radiation or scattering problems involving structures that either have large electrical dimensions or fine features. The characterizing key features of these CEM frameworks are twofold:

(i) Compression of the original MoM matrix equation by employing relatively few macro basis functions (MBFs) in order to exploit the low degrees-of-freedom (DoFs) that the physics-based equivalent current effectively attains, and reducing both the memory storage requirements and solve-time significantly.

(ii) Computation of the coupling between spatially (or spectrally) distant MBFs in order to construct the reduced MoM matrix in a time-efficient manner.

The objective of these CEM frameworks is to retain the low-order basis functions of high spatial resolution for the current (with minimum cell size $\lambda/10$) to be able to conform to arbitrarily shaped geometries, while reducing the DoFs for the current by employing MBFs. They present the additional advantage that existing MoM codes can be reused with only minor modifications. Within the MBF-type class of methods, one can recognize three widely-published CEM modeling frameworks. These are:

- **The Characteristic Basis Function Method (CBFM, [6])** which has been successfully applied to a large class of scattering [8], radiation [9], absorbing [10], as well as to waveguide and transmission line problems [11], [12]. Applications to planar antenna and microwave circuits have been described in [13]. This has been done typically by employing plane-wave-spectrum (PWS) generated CBFs for scattering problems (Sec. IV-A, and [14]), and primary, secondary or tertiary CBFs for radiation problems (Sec. IV-C), or a combination thereof [15]. CBFs partially overlap to preserve the continuity between electrically interconnected subdomains [16], and subdomain extension and windowing techniques are used to mitigate edge-truncation effects when generating CBFs on the interconnected subdomains (Sec. IV-A). CBF interactions for widely spaced subdomains have been computed rapidly, either using the Adaptive Cross Approximation (ACA) Algorithm (Sec. V-A, and [16]), an MBF-field interpolation technique (Sec. V-B, and [17]), or the Multilevel Fast Multipole Algorithm (MLFMA, [18]). The CBFM has shown to be highly paralellizable [19], [20], and a multilevel version of the CBFM has been described in [21], [22] and will be revisited in Sec. VII.
- **The Synthetic-Functions Approach (SFX, [7])** applies the singular value decomposition (SVD) along with a thresholding procedure on the singular values to the

initially generated set of MBFs in order to orthonormalize and to retain only a minimum number of MBFs [23]. The SFX typically generates MBFs using point sources that surround the subdomain under excitation (Sec. IV-B). Furthermore, the SFX employs a separate and independent set of low-order subsectional basis functions across the subdomain interfaces to electrically interconnect subdomains [24]. Far MBF interactions have been computed rapidly through an AIM approach (Sec. V-D, and [25]). It has primarily been applied to solve radiation problems [24], [26] and has also been hybridized with a multi-resolution approach [27].

- **The Macro Basis Function Method [5]**, which employs MBFs obtained from both spectral (Sec. IV-D, and [28]) and spatial domain analyses. Both domains are also exploited for efficient computation of reaction integrals between distant MBFs (see for instance the multipole approach both in Sec. V-C and [29], or the spectral domain approach in [30]). The method has been applied to both regular and irregular antenna arrays [31]. As mentioned in Sec. VI, closer inspection of iterative and MBF-based formulation has revealed an equivalence between specific types of MBF generation procedures and Krylov subspace iterative techniques, such as the Full Orthogonalization Method (FOM) [32]. Besides, a relationship has been established between the use of a block-diagonal preconditioner and the use of partially overlapping MBFs in iterative and iteration-free approaches [33].

Other more or less related subdomain-decomposition methods are the Sub-Entire-Domain Basis Function Method (SED) [34], the Linear Embedding via Green's Operators (LEGO) technique combined with the eigencurrent approach [35], [36], and a specific MBF domain decomposition technique, as described in [37].

IV. MBF Generation

MBF-type approaches rely, for different subdomains, on an *a priori* choice of the subpsace in which the solution is expected to reside. This subspace is described by the MBFs, whose choice is therefore crucial to obtaining accurate solutions. We describe below different methods that have been developed toward this end.

A. Plane-wave spectrum

The *plane-wave spectrum* approach [14], [38] calculates the current induced on each subdomain due to any electromagnetic field radiated by a source external to the domain. If the *far-field condition* is assumed, then the external field can be expanded in terms of a series of plane waves in the visible spectrum. Thus, according to the *superposition principle*, any induced current can be represented as a linear combination of the currents induced by the set of plane waves. For the m-th domain, the procedure can be mathematically expressed as

$$\mathbf{J}_m = \mathbf{Z}_{mm}^{-1}\mathbf{P}_m, \tag{3}$$

where $\mathbf{P}_m$ is a matrix whose columns are the coefficients of the incident plane-wave field tested by the low-level basis functions in the m-th domain; $\mathbf{Z}_{mm}$ is the impedance matrix comprised of the reaction terms between low-level basis functions in the m-th domain.

In general, equation (3) is modified to consider *extended subdomains* [14], [38]. The purpose of this extension is twofold. First, the edge effect due to the domain truncation is moved away and, second, it enables us to include the near-field contributions of the region closest to the domain.

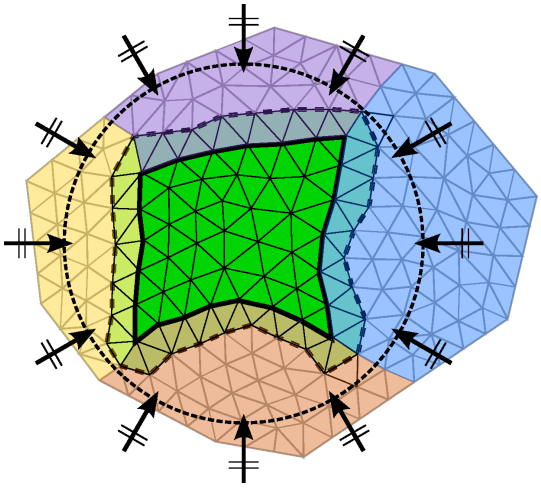

Fig. 1. MBFs generation based on the plane-wave expansion.

Fig. 1 illustrates this approach. The continuous thick trace shows the boundary of the domain in which the MBFs are being generated whereas the dotted thick trace delimits the extended domain wherein the currents induced by each plane wave are calculated.

After discarding the currents in the extension, the computed currents are filtered using the *singular value decomposition*, which yields the final set of MBFs and guarantees the orthogonality between the MBFs. Thus, the SVD entails the following matrix factorization:

$$\mathbf{J}_m = \tilde{\mathbf{Q}}_m \mathbf{\Sigma}_m \mathbf{V}_m^H, \tag{4}$$

where the diagonal of the matrix $\mathbf{\Sigma}_m$ contains the singular value of the decomposition. The final MBFs coefficients $\mathbf{Q}_m$ are calculated by retaining only the columns in $\tilde{\mathbf{Q}}_m$ whose normalized singular value is above a prescribed threshold τ. Hence, the i-th column is only retained if $\sigma_i/\sigma_1 > \tau$. Typical values for this threshold ranges from 10^{-3} to 10^{-5}.

The plane-wave spectrum approach typically yields a higher number of MBFs as compared to the previous approaches. However, the computed MBFs do not depend on the excitation. Consequently, it is usually preferable to analyze problems that involve multiple excitation sources, as for example in *monostatic RCS* computations. A modification of this approach is to employ spherical waves instead of plane waves, as suggested in [10].

B. Point sources

Another approach for generating the MBFs consists of replacing plane waves by a number of point sources distributed over a given surface that surrounds the subdomain of interest

[39]. This approach may be regarded as relying on the surface equivalence principle, according to which the sources external to the surface can be replaced by equivalent electric and magnetic currents on the surface [40]. In addition, for spherical surfaces, the equivalent current can be limited to electrical currents only. Such equivalent currents, in principle, ensure the completeness of the MBF basis formed in this way. The main reason why the base may not be truly complete in practice is the limited sampling of the equivalence surface. This may become an issue when the surface very closely wraps the subdomain of interest, and the approach becomes virtually impractical when the subdomains are connected, since it then becomes difficult to let the equivalence surface partition the subdomains, unless the equivalence surface entirely includes the extended subdomain introduced in the previous section.

C. Primary and secondary MBFs

Another way of generating the MBFs uses primary and secondary current distributions [9]; it is particularly suitable (but not limited) to the analysis of antenna arrays. Indeed, for the analysis of mutual coupling in arrays, it is generally sufficient to provide all the embedded element patterns as well as the array impedance matrix. The above quantities can be obtained from the solutions derived by exciting the array at each of the individual ports. The construction of MBFs may then be obtained from the excitation of the antenna in isolation, followed by the excitation of the other elements by the fields radiated by the first element. From the MoM point of view, this solution is obtained by multiplying blocks of the MoM impedance matrix. More precisely, the primary MBF on domain i corresponds to $\mathbf{f}_{p,i} = \mathbf{Z}_{ii}^{-1}\,\mathbf{v}_i$, where $\mathbf{v}_i$ is the excitation vector on antenna (or subdomain) i, while a secondary MBF on antenna j is obtained from the equation $\mathbf{f}_{s,j} = \mathbf{Z}_{jj}^{-1}\,\mathbf{Z}_{ji}\,\mathbf{f}_{p,i}$. In order to enrich the set of MBFs, it is logical to employ the primary and secondary MBFs on all antennas, by considering every possible excitation, or at least secondary MBFs created from primaries on every neighboring subdomain. This approach usually provides excellent results on arrays of disconnected elements. For arrays of connected elements, combining this idea with the use of extended subdomains, has proven to be very efficient and accurate, as has been explained in Sec. IV.A.

The idea of primary and secondary MBFs can be extended to higher multiple-scattering orders, by including the tertiary MBFs as done for instance in [41], [42] and [43]. There is virtually no limit to the orders that can be considered, albeit at an increased computational cost. As explained in Section VI, the completeness of MBFs bases can, in principle, be achieved by considering virtually unlimited orders (i.e., only limited by the number of unknowns in the problem), though this is not a viable option in practice. Fortunately, very high accuracy can be achieved with orders limited to 2 or 3, especially when extended subdomains are used. In [33], the somewhat complex process of domain extension has been made implicit by first pre-conditioning the system of equations. The preconditioner utilized is a nearest-interaction preconditioner, which can be regarded as an extension of the shield-block preconditioner introduced in [44]. In a nutshell, an extension S_{i^a} is associated with each subdomain S_i in this approach (see Fig. 1). In the following, segments of vectors and blocks of matrices will be associated with different subdomains and their extensions by using indices i and i^a, respectively. The preconditioned system of equations then reads $\mathcal{Z}\,\mathbf{x} = \mathbf{w}$, with the following definitions:

$$\mathbf{w}_i = \mathbf{Y}_i\ (\mathbf{v}_i - \mathbf{P}_i\,\mathbf{v}_{i^a}) \tag{5}$$

with $\mathbf{v}_i$ and $\mathbf{v}_{i^a}$ corresponding to segments of the original excitation vector, and

$$\mathbf{P}_i \;=\; \mathbf{Z}_{i,i^a}\ \mathbf{Z}_{i^a,i^a}^{-1} \tag{6}$$

$$\mathbf{Y}_i \;=\; (\mathbf{Z}_{i,i} - \mathbf{P}_i\,\mathbf{Z}_{i^a,i})^{-1} \tag{7}$$

$$\mathcal{Z}_{i,j} = \mathbf{Y}_i\ (\mathbf{Z}_{i,j} - \mathbf{P}_i\,\mathbf{Z}_{i^a,j}) \tag{8}$$

There are two reasons for doing this. First, the preconditioned system of equations ensures faster convergence of Krylov-based iterative techniques. Second, MBFs of order n can be obtained simply through multiplication to the left of a primary MBF by a number of consecutive matrices. By "consecutive" we mean that a matrix with first index k must be multiplied to the left by a matrix with second index k. In Section VI, it will be shown how such MBFs can be combined to construct Krylov subspaces, in which solutions are sought in iterative schemes.

D. ASM-MBF

The ASM-MBF approach is limited to regular arrays of antennas or scatterers [45]. For array problems, one seeks the solutions (current or field distributions) over the entire array when an arbitrary element is excited. Therefore, it makes sense to obtain the MBFs from the field or current distribution in an infinite array when a single element is excited. As explained in [46], this problem can be solved as the superposition of infinite-array problems (with all elements excited) by scanning through every possible inter-element phase shift. In one dimension, this is expressed as:

$$\vec{J}_m = \frac{1}{2\pi}\int_0^{2\pi} \vec{J}^{\infty}(\psi)\,e^{-j\,m\,\psi}\,d\psi \tag{9}$$

where $\vec{J}_m$ is the current on element m when element 0 is excited, and $\vec{J}_m^{\infty}(\psi)$ is the infinite-array current at the same position within the unit cell, for an inter-element phase shift equal to ψ. By superposition, the current distributions obtained on successive elements when a single element is excited forms an excellent basis for an arbitrary excitation law. Even the effects of array truncation can be well represented in this basis, since currents "reflected" by the edges of the array may form current distributions that are very similar to those obtained from "direct" waves launched by a single element in the infinite array. This might not hold true for elements located right at the edges (or corners) of the array, in particular when the elements are complex and connected with each other. Therefore, to improve the accuracy, a few current distributions, obtained in a 2×2 array, are added to the set of MBFs.

It has been found that this approach leads to a very fast convergence of the solution w.r.t. the number of points used

to discretize the ASM integration, and excellent accuracy has been realized using about 20 MBFs per element. More importantly, for the reasons explained above, the MBFs obtained in this manner are excitation-independent. An open-source Matlab software for the example of linear dipole arrays has been described in [47]. An extension of this methodology for arrays of plasmonic rods has been detailed in [48].

V. Fast MBF interactions

The construction of the reduced matrix equation in (1) requires us to compute many blocks of the form

$$\mathbf{Q}_m^H \, \mathbf{Z}_{mn} \, \mathbf{Q}_n \tag{10}$$

and it is desirable to perform this computation in a time-efficient manner. From a physics point-of-view, the factor $\mathbf{Z}_{mn}\,\mathbf{Q}_n$ represents the excitation matrix $\mathbf{V}_{mn}$ due to the source MBFs on the nth subdomain, whose radiated E-fields are tested on the mth subdomain. As the source and observation subdomains become electrically well-separated in free space, the DoFs of any such subdomain excitation vector (column of $\mathbf{V}_{mn}$) reduces. In fact, for extremely large separation distances, each excitation vector practically represents a single incident plane wave field (thus only one DOF, or one mode). One can exploit this phenomenon to rapidly compute (10), either through a field expansion method employing only the first few dominant modes, or by using an algebraic method exploiting the low-rank nature of $\mathbf{Z}_{mn}$.

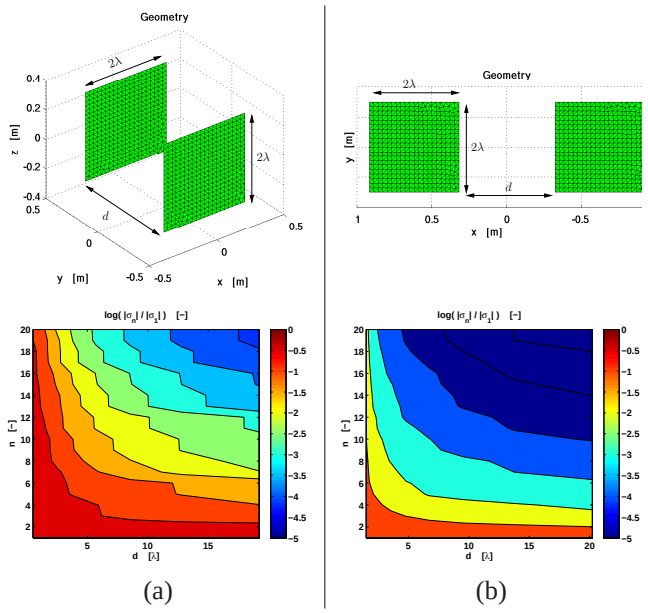

(a) (b)

Fig. 2. Normalized singular value spectrum $\log_{10}(|\sigma_n|/|\sigma_1|)$ of the coupling matrix block $\mathbf{Z}_{mn}$ between a pair of $2\lambda \times 2\lambda$ plates ($\lambda/10$ meshing, 2320 RWGs in total), as a function of their separation distance d when (a) facing each other, and; (b) in a side-by-side configuration.

As regards the rank-deficiency of $\mathbf{Z}_{mn}$, Fig. 2(a) and (b) show how the singular value spectrum of $\mathbf{Z}_{mn}$ depends on the separation distance d between a pair of $2\lambda \times 2\lambda$ plates. Note that, when defining the effective numerical rank as $r = \text{rank}(\mathbf{Z}_{mn}) = |\sigma_r|/|\sigma_1| = 10^{-2}$, i.e., when r is the number of singular values that are within 10^{-2} from the largest singular value, one can observe how r decreases as a function of d [*cf.* yellowish region in Fig. 2(a)]. For $d = 10\lambda$, the effective rank is $r \approx 10$, which is less than 0.5% of an equally large full-rank matrix. It is also observed that the effective rank decreases even faster for plates that are placed side-by-side. For instance, for $d = 10\lambda$, we find that $r \approx 4$, which is smaller than 0.1% of an equally large full-rank matrix. Clearly, both the subdomain sizes and orientation play an important role in the degree of rank-deficiency of $\mathbf{Z}_{mn}$ and, consequently, on the computation time of the reduced matrix elements in (1).

A. The Adaptive Cross Approximation (ACA) algorithm

The Adaptive Cross Approximation (ACA) algorithm, originally developed by Bebendorf [49], approximates the $N_m \times N_n$ rank-deficient matrix block $\mathbf{Z}_{mn}$ through the low-rank block factorized matrix $\widetilde{\mathbf{Z}}_{mn} = \mathbf{U}_m^{N_m \times r} \mathbf{V}_n^{r \times N_n}$. This is advantageous because (10) can then be computed rapidly using a minimum number of multiplications as

$$(\mathbf{Q}_m^H \, \mathbf{U}_m)(\mathbf{V}_n \, \mathbf{Q}_n). \tag{11}$$

A very important feature of the ACA algorithm is that the matrices $\mathbf{U}_m$ and $\mathbf{V}_n$ are constructed on-the-fly, without *a priori* knowledge of the entire original matrix block $\mathbf{Z}_{mn}$; the iterative ACA algorithm dynamically selects certain rows and columns of $\mathbf{Z}_{mn}$ and, in conjunction with a normalization procedure, these normalized vectors form the rows and columns of the matrices $\mathbf{V}_n$ and $\mathbf{U}_m$, respectively. Indeed, for well-separated groups of RWGs (Rao-Wilton-Glisson double-triangle basis functions), the electric field at the observation group m produced by any source RWG can be expressed as a linear combination of the fields produced by only a few of these source RWGs (source sampling). Likewise, the electric field tested at the observation group m produced by any source RWG can be expressed as a linear combination of the fields tested by only a few of these observation RWGs (field sampling). Hence, a cross-approximation technique can be used to adaptively construct the subsets of relevant source and observation RWGs.

The ACA algorithm is purely algebraic in nature, easy to implement, and can be used irrespectively of the kernel of the integral equation, basis functions or type of integral equation formulation. The ACA algorithm has not only been applied to solve low-frequency EMC problems [50], but also to solve electrodynamic antenna problems involving oscillatory kernels using an MBF approach [16]. Since the ACA algorithm approximates $\mathbf{Z}_{mn}$ through the product $\mathbf{U}_m\mathbf{V}_n$, most of the non-selected elements of $\mathbf{Z}_{mn}$ are predicted through linear interpolation, i.e., from the product $\mathbf{U}_m\mathbf{V}_n$; hence, the time-harmonic nature of the fields is not accounted for. The ACA algorithm may therefore require more iterations than a more physics-based approximation technique, such as the multipole approach as explained below. Also, the computational overhead of the ACA algorithm becomes excessive for a relatively large numerical rank of $\mathbf{Z}_{mn}$ (e.g., for small subdomain separation distances), so that a direct element-by-element computation of $\mathbf{Z}_{mn}$ is more efficient. The interested reader may refer to [50], where a pseudo-code of the ACA algorithm in Matlab notation can be found.

Fig. 3 shows the matrix fill-time of the ACA algorithm for building the matrices $\mathbf{U}_m$ and $\mathbf{V}_n$ – when applied to the case shown in Fig. 2(a) – relative to the time needed when a direct matrix filling approach is used for building $\mathbf{Z}_{mn}$. It is

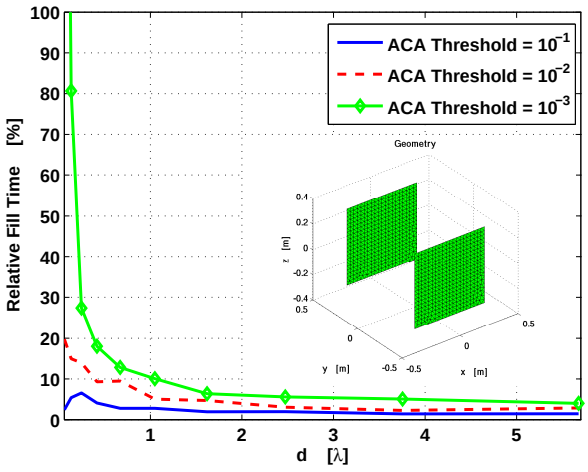

Fig. 3. Fill time of the ACA constructed matrix blocks $\mathbf{V}_n$ and $\mathbf{U}_m$, relative to a full element-by-element filling approach of $\mathbf{Z}_{mn}$, as a function of the separation distance d for a pair of plates facing each other [*cf.* Fig. 2(a)].

evident from Fig. 3 that the speed advantage of the ACA over a direct matrix filling technique is significant. For instance, for $d > 0.5\lambda$, the ACA algorithm requires less than 15% of the time needed to fill a full MoM block on an element-by-element basis. This is true even for ACA thresholds as low as 10^{-3}, which means that the relative ACA approximation error $\|\mathbf{V}_n\mathbf{U}_m - \mathbf{Z}_{mn}\|_{\mathrm{F}}/\|\mathbf{Z}_{mn}\|_{\mathrm{F}} < 10^{-3}$, where $\|\cdot\|_{\mathrm{F}}$ denotes the Frobenius norm. Hence, for electrically large problems, the average ACA matrix fill time typically takes only a few percent of that needed in a direct matrix filling approach. As an alternative to the ACA technique, matrix compression based on the incomplete QR decomposition [51] has been used in [33].

B. Tested field interpolation

Another technique, which also exploits the DoF of the field radiated by the MBFs, is based on the conventional interpolation of the radiated field [17]. Thus, the tested field can be computed by calculating the field in a small grid over the observation domain and, then, retrieving the field in the low-level basis functions via interpolation. Fig. 4 shows this interpolation scheme for a planar geometry.

In order to rapidly compute the field radiated by each MBF in the n-th source domain over the m-th observation domain, the matrix $\tilde{\mathbf{V}}_{mn}$ relating the coefficients of the source domain MBFs and the p-component of the field ($p = x, y$ or z) in the interpolation grid are computed. By invoking the reciprocity theorem, the entries of this matrix can be expressed as [17]:

$$\tilde{\mathbf{V}}_{mn}[i,j] = \int \boldsymbol{f}_{n,j} \cdot \boldsymbol{E}_T(\boldsymbol{r}_{m,i}) dS, \qquad (12)$$

wherein $\boldsymbol{r}_{m,i}$ is the i-th observation point in the interpolation grid for the m-th MBF domain; $\boldsymbol{E}_T(\boldsymbol{r})$ is the field radiated

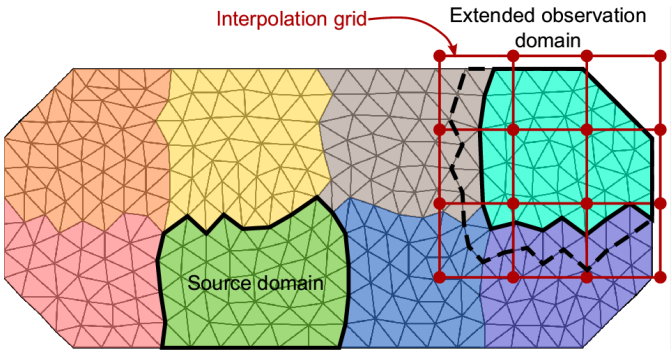

Fig. 4. Interpolation grid for fast computation of the reduced matrix.

by an infinitesimal dipole at the spatial point $\boldsymbol{r}$ and oriented along the p-axis; and, $\boldsymbol{f}_{n,j}$ is the j-th low-level basis function in the n-th MBF domain. Once these matrices have been computed, the field in the sampling grid can be calculated by post-multiplying with the MBF coefficients $\mathbf{E}_{mn}^{grid} = \tilde{\mathbf{V}}_{mn}\mathbf{Q}_n$. Thus, the need for computationally expensive integrations in the source domain is obviated. It is remarkable to note that this approach is compatible with more advanced interpolation schemes such as those proposed in [52] wherein a phase extraction is carried out first to further reduce the DoFs.

The interpolation scheme is illustrated by means of the example shown in Fig. 4 where the bistatic analysis of two square plates with edge lengths of 2λ is considered. Both plates lie in the same plane and the distance between them is 1.5λ. The frequency is chosen to be 300MHz. For this case, the interaction between both blocks is calculated by using a 9x9 interpolation grid, which enables one to reduce the time to compute the reaction term between the MBFs of both plates from 4.28s to 0.37s. We note an excellent agreement in the entire dynamic range of the bistatic RCS.

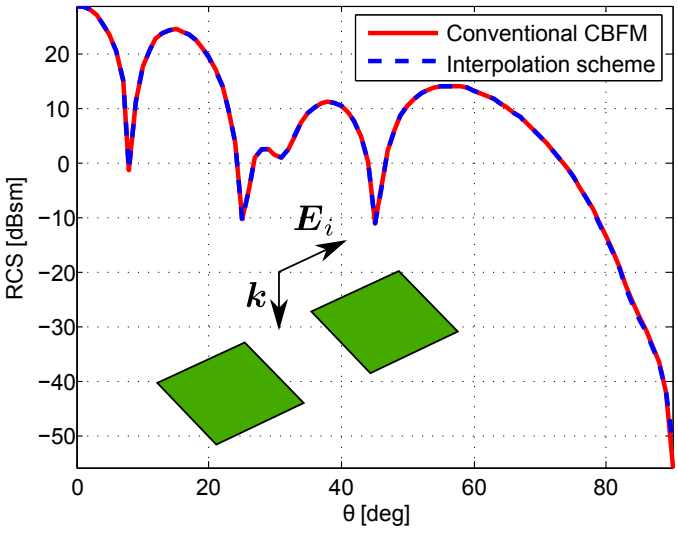

Fig. 5. Bistatic RCS between two square plates with a distance of 1.5λ and edges equal to 2λ.

Another approach involving interpolation for estimating MBF interactions is described in [53]. It has been developed for the analysis of irregular arrays of identical antennas (or

scatterers) and it produces a very simple model for the interactions between MBFs versus relative position. It is based on three physical transformations: far-field extraction, phase removal and change of the distance variable. In this way, a harmonic-polynomial model is obtained, valid for any relative position in the plane, through the explicit calculation of interactions at a few tens of relative positions.

C. Spectral approaches

Interactions between subdomains can be speeded up by exploiting integral representations of the scalar Green's function. This is particularly fast when, in such representations, the dependence on source and observation coordinates is separable. In practice, the separable form is generally identified with a plane wave, expressed by a complex exponential. Two categories of spectral approaches have been developed in the literature. The first one is associated with multipole decompositions, while the second one is associated with waves radiated from a given reference plane.

a) Multipole approach: The derivation of this approach is provided in [29]. The final result reads as follows. If $\vec{F}_t$ is the radiation pattern of a conjugated Macro Testing Function and $\vec{F}_b$ is the radiation pattern of a conjugated Macro Basis Function, the interaction between them can be written:

$$I = \iint \vec{F}_t^{\star} \,.\, \vec{F}_b \, T(k, \vec{r}, \hat{u}) \, dU \qquad (13)$$

where $T(\hat{u})$ is the translation function appearing in multipole decompositions, within a constant factor, k is the free-space wavenumber and $\vec{r}$ is the vector distance between reference points of the source and observation domains. The integration domain U corresponds to the unit sphere, to which the unit vector $\hat{u}$ points. This approach allows the computation of the interactions between subdomains without computing the interaction matrix $\mathbf{Z}_{ij}$. The only constraint is that the distance between subdomains should exceed a certain minimum, whose value is of the order of half wavelength. Fig. 7 illustrates the accuracy of the multipole-based method with 40×40 integration points over the unit sphere, for the antenna shown in Fig. 6. The MBF considered is a primary (direct excitation of one antenna); the solid line provides the magnitude of the interaction versus distance in wavelengths, while the dashed line povides, on the same log-scale, the magnitude of the difference between results obtained using the MoM matrix approach described in Section 2 on one side, and the multipole approach on the other side. It can be seen that the quality suddenly degrades for very small distances. However, this sudden change happens when the antennas are nearly touching each other. More precisely, if the acceptable threshold is defined at a 1 % error level, then for the 5 cm wavelength, the tip-to-tip distance between antennas should be at least 0.5 cm, while that distance is only 0.2 cm for the 2.5 cm wavelength case.

If N is the number of elementary basis functions on a given subdomain, the complexity of computing interactions between the MBFs is typically reduced from N^2 to N. Assuming sudomains of the order of one wavelength and a relatively coarse mesh; the time saving is smaller for larger domains and larger for finer meshes. Such time-saving has been demonstrated in the case of arrays of broadband conducting antennas in [29], and has been extended in [32] to subdomains made of penetrable bodies. An extension to printed antennas is described in [54]. In the latter case, the Green's function is decomposed into a spherical wave, related to an average-medium term, as well as into cylindrical waves [55]. In both cases, the MBF interactions are computed using multipoles. The treatment of the terms related to the cylindrical waves has been described above. For the multipole-based treatment of the terms related to the cylindrical waves, the complexity is proportional to $N^{1/2}$ where N is the number of elementary basis functions per antenna, and to the number of cylindrical waves needed, which is typically in the order of 10. For this case, the computation time for printed structures is only marginally larger than what it is when the subdomains are interacting in free space.

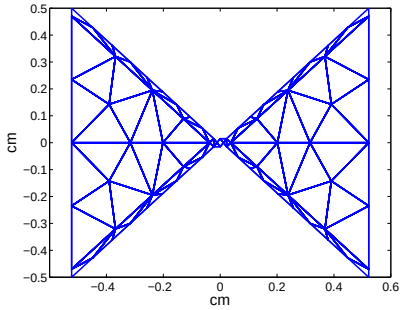

Fig. 6. Discretization of the bowtie antenna considered in the multipole analysis of figure 7.

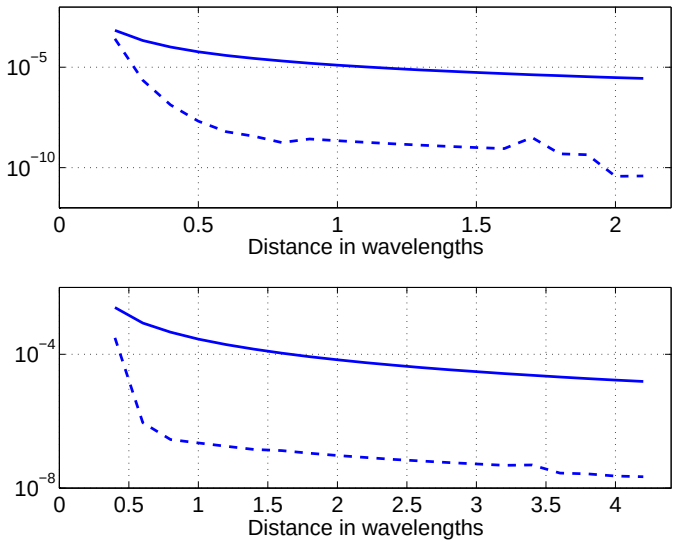

Fig. 7. Interactions (solid) between primary MBFs defined on a pair of antennas versus center-to-center distance (vertical shift in Fig. 6). Dashed: error incurred by multipole-based approach. Top: 5 cm wavelength. Bottom: 2.5 cm wavelength.

b) Waves from a reference plane: Assuming a reference plane XY, the scalar Green's function can be written as a continuous spectrum of plane waves, characterized by their

lateral wavenumbers k_x and k_y. If $k_x^2 + k_y^2 < k^2$, then the plane wave is propagating along z, otherwise it is evanescent. Using such a decomposition, the interactions between MBFs can be written as

$$I = K \iint \mathbf{f}_t \, e^{-j\,(k_x\,\Delta_x + k_y\,\Delta_y)} \, \mathbf{f}_b^{\star} \, \underline{\underline{\mathbf{G}}}(k_x, k_y)\, dk_x\, dk_y \quad (14)$$

where $\mathbf{f}_t$ and $\mathbf{f}_b$ are the Fourier transforms, or "patterns", of MTFs and MBFs in direction $(k_x, k_y, k_z)/k$, which becomes complex outside the unit circle in the $(k_x, k_y)/k$ plane; Δ_x and Δ_y are distances between reference points of the subdomains in the XY plane; $\underline{\underline{\mathbf{G}}}$ is the spectral-domain representation of the dyadic Green's function and K is a constant. Such an approach, specialized to analytically-derived CBFs, has been presented in [56]. Since the MBFs are defined over domains that are substantially larger than those of elementary basis functions, their pattern is relatively narrow; hence the integration domain in wavenumber space can be strongly reduced. Examples of this approach are given in [30] in the case of printed antennas.

D. FFT-based approach

In [57], the interactions between MBFs are obtained using the AIM for printed structures. This may be viewed as a fast spectral approach, since the space-domain convolution between MBFs, MTFs and the Green's function are written as products in spectral domain. In that approach, forward and backward 3D FFTs are exploited to compute the space-to-spectral and spectral-to-space domain transforms. This may be regarded as one of the most effective MBF-interaction approaches to date. Reference [57] also provides expressions for the complexities of the different interactions techniques as well as validations for large problems, such as arrays of printed antennas.

VI. Relation With Krylov Sub-Space Iteration

A. Reformulation of Krylov iterations

As reminded in Section II, the concept of Macro Basis Functions can be expressed in a relatively compact form. Krylov subspace techniques, essentially developed in the seventies, are also based on a few key ideas, some of which also appear in MBF methods.

However, the use of specific tools, as for instance the properties of Hessenberg matrices resulting from the Arnoldi orthogonalization process [58], may somewhat obscure the basic ideas behind Krylov methods. In this section, we propose an alternative –or perhaps simplistic– formulation for two popular Krylov-based methods, namely the FOM (Full Orthogonalization Method) and GMRES (Generalized Minimal Residual), both of which are described in the seminal paper by Saad and Schulz [59], published in 1986. As explained further below, that alternative formulation may incur a very marginal reduction of efficiency. However, the formulation proposed here should further clarify the relationship between Krylov subspace iterative techniques and the MBF approach. This will be explained below in two steps.

First, let us assume a relatively well preconditioned system of equations $\mathbf{A}\,\mathbf{x} = \mathbf{b}$, with $\mathbf{A}$ sufficiently close to a unit matrix. The reader is referred to [58] for more precise figures of merit of preconditioning and to [60] for recent advances regarding preconditioning in the framework of integral-equation solution in high-frequency electromagnetics. For the above system of equations, with $\mathbf{x}_0$ as an initial guess, the first residual is $\mathbf{r}_0 = \mathbf{b} - \mathbf{A}\,\mathbf{x}_0$ and the simplest possible iteration [58] is obtained by considering at iteration k a correction equal to the residual $\mathbf{r}_{k-1}$; hence $\mathbf{x}_k = \mathbf{x}_{k-1} + \mathbf{b} - \mathbf{A}\,\mathbf{x}_{k-1}$. As compared to $\mathbf{x}_{k-1}$, $\mathbf{x}_k$ has high chances to be closer to the exact solution $\mathbf{x}_{k-1} + \mathbf{A}^{-1}(\mathbf{b} - \mathbf{A}\,\mathbf{x}_{k-1})$, because $\mathbf{A}$ is relatively close to a unit matrix, as a result of preconditioning. The convergence of this procedure is dictated by the eigenvalues of the iteration matrix $(\mathbf{I} - \mathbf{A})$, which are unfortunately not known *a priori*. As has been very well summarized in [61], Krylov iteration essentially consists of keeping all the approximants obtained up to the step k and to recombine them to obtain a more accurate solution. This is equivalent to searching $\mathbf{x'} = \mathbf{x} - \mathbf{x}_0$ in the subspace spanned by the successive residuals $\mathbf{r}_0$, $\mathbf{r}_1$, etc. Based on the above, it is easy to prove that this subspace can also be written as $\mathrm{Span}\Big\{\mathbf{r}_0, \mathbf{A}\,\mathbf{r}_0, \mathbf{A}^2\,\mathbf{r}_0, ..., \mathbf{A}^{k-1}\,\mathbf{r}_0\Big\}$, which is the Krylov subspace of order k. Each of the vectors $\mathbf{s}^{(q)} = \mathbf{A}^{q-1}\,\mathbf{r}_0$ describing this subspace, which we will name the *generating vectors*, may be regarded as MBFs spanning the whole computational domain. In the following, we will denote by $\mathbf{Q}$ the matrix whose columns are formed by using the consecutive generating vectors.

Second, one needs to establish a set of conditions which will determine the scalar coefficients $y_0 ... y_{k-1}$ that multiply each generating vector in the final estimate of $\mathbf{x}$, so that we can write $\mathbf{x'} = \mathbf{x} - \mathbf{x}_0 \simeq \mathbf{Q}\,\mathbf{y}$. In passing, to avoid dealing with the initial guess $\mathbf{x}_0$, the system of equations may be rewritten as $\mathbf{A}\,\mathbf{x'} = \mathbf{r}_0$. A simple approach for finding the vector of coefficients $\mathbf{y}$ consists of testing the original system of equations with the generating vectors, i.e by using

$$\mathbf{Q}^H\,\mathbf{A}\,\mathbf{Q}\,\mathbf{y} = \mathbf{Q}^H\,\mathbf{r}_0 \quad (15)$$

This is mathematically equivalent to the Full Orthogonalization method (FOM, [59]), which imposes the residual to be orthogonal to the Krylov subpsace, and hence to each generating vector $\mathbf{s}^{(q)}$ composing $\mathbf{Q}$. This also has the same form as an MBF approach performed over a single domain. The reduced system of equations obtained in this way will in general be ill-conditioned, because of quasi-linear dependence between generating vectors. This is why it is necessary to orthogonalize the generating vectors composing $\mathbf{Q}$. This can be achieved using the Arnoldi procedure, inspired from the Gram-Schmidt method. As compared to (15), an alternative approach consists of testing the initial system of equations with the generating vectors, each left-multiplied by matrix $\mathbf{A}$. This may be written as

$$(\mathbf{A}\,\mathbf{Q})^H\,(\mathbf{A}\,\mathbf{Q})\,\mathbf{y} = (\mathbf{A}\,\mathbf{Q})^H\,\mathbf{r}_0 \quad (16)$$

which may be viewed as the normal equation which minimizes the residual $\mathbf{A}\,\mathbf{x'} - \mathbf{r}_0$ in the least-squares sense. This is equivalent to the GMRES approach [59].

In practice, the above methods can be implemented as follows. As the consecutive generating vectors $\mathbf{A}^k\,\mathbf{r}_0$ are created, they are orthogonalized and placed into matrix $\mathbf{Q}$. At every step, the following system of equations is solved: $\mathbf{B}^H\,\mathbf{A}\,\mathbf{Q}\,\mathbf{y} = \mathbf{B}^H\,\mathbf{r}_0$, with $\mathbf{B} = \mathbf{Q}$ for FOM and $\mathbf{B} = \mathbf{A}\,\mathbf{Q}$ for GMRES. The solution is then given by $\mathbf{x} = \mathbf{x}_0 + \mathbf{Q}\,\mathbf{y}$, The $\mathbf{A}\,\mathbf{Q}$ vectors can be computed at very low cost, based on operations already carried out to build the Krylov subspace. This observation makes it possible to use only one matrix-vector product per iteration instead of two. The simplicity of this new formulation may incur a slight extra computational cost. Indeed, standard implementations of FOM and GMRES make use of the Hessenberg matrix [59] resulting from the Arnoldi procedure used to orthogonalize the Krylov subspace. It is an upper-triangular matrix with an extra non-zero diagonal below the main diagonal (it is related to the $\mathbf{R}$ matrix resulting from the modified Gram-Schmidt procedure). Consecutive solutions of the larger problems obtained at each iteration can be accelerated by keeping in memory previous pivoting operations on the growing Hessenberg matrix. However, as long as the number of iterations is much smaller than the number of unknowns (say by at least one order of magnitude), the solution time of the reduced system of equations is not the limiting factor. The dominant part of the computational effort is associated with the product between matrix $\mathbf{A}$ and consecutive generating vectors. Under those circumstances, the simple procedure proposed here is, in practice, equally efficient.

When the number of iterations becomes large, the generating vectors may require too much memory and their orthogonalization may become too expensive (linear growth per iteration). Also, they may lead to poor conditioning because they are only marginally linearly independent, a problem that can get exacerbated by numerical roundoff. Then, the iteration may be restarted, considering the solution obtained after a number of iterations as the new first guess.

B. Relation between Krylov iteration and MBF approach

Regarding MBF construction, a particularly well-posed approach consists of using "primary" and "secondary" MBFs [9], extended to higher orders in [41]. In a nutshell, the current distribution obtained on a given subdomain impresses fields on another subdomain, in which currents are induced when that other subdomain is taken in isolation; this process is continued in a multiple-scattering approach. Let us denote by S_i the subdomain of interest and by S_j all the other subdomains. If the currents on other subdomains are known exactly, then the MBFs they induce on subdomain S_i form a complete set, with known coefficients. This can be proven from the i-th block-line of the system of equations, which represents the testing of fields on S_i. If the $\mathbf{Z}_{ij}$ matrix denotes blocks of the system matrix, $\mathbf{x}_j$ denotes solutions on S_j and $\mathbf{v}_j$ the segment of the excitation vector standing for testing of incident fields on S_i, then the multiple-scattering process produces the following general solution on S_i:

$$\mathbf{x}_i = \mathbf{Z}_{ii}^{-1}\,\left(\mathbf{v}_i - \sum_{j\neq i}\alpha_j \mathbf{Z}_{ij}\,\mathbf{x}_j\right) \tag{17}$$

where the $\mathbf{Z}_{ii}^{-1}\,\mathbf{Z}_{ij}\,\mathbf{x}_j$ terms are the secondary MBFs and the α_j coefficients are yet to be determined. It is also obvious from the i-th block-line of the system of equations that an exact solution for $\mathbf{x}_i$ can be obtained with $\alpha_j = 1$ for all j's if the $\mathbf{x}_j$'s are known *a priori*. Of course, this condition sounds difficult to satisfy; however, in common with the Krylov-based approaches, the fact of keeping free all the coefficients that multiply the generated MBFs provides important degrees of freedom (DoFs). To a large extent, those DoFs may compensate for the deficiency of working with MBFs generated from inaccurate current distributions $\mathbf{x}_j$ on the subdomains S_j. More DoFs are obtained by adding higher-order multiple-scattering MBFs, as explained in Sec. IV.C.

Two challenges appear when implementing the above procedure. First, in a multiple-scattering process, the number of generated MBFs increases exponentially. Second, connected subdomains may lead to non-physical MBFs on S_i, with nearly-singular current distributions along the contour of S_i. To circumvent the latter problem, several authors [62], [63] opted to extend subdomain S_i (see also Sec. IV.A), with a connected auxiliary subdomain S_i^a and to retain as an MBF the current induced only on subdomain S_i (see Figs. 1 and 2). As already mentioned in Section IV, in [33], it is proven that this approach is equivalent to the classical MBF approach (i.e., without subdomain extensions), provided that the system of equations is modified using a nearest-interactions preconditioner, which may be viewed as an extension of the shielded-block preconditionner proposed in [44] for disconnected periodic structures. We will denote by $\boldsymbol{\mathcal{Z}}\,\mathbf{x} = \mathbf{w}$ the system of equations preconditioned in this manner. Details about the combination of this preconditioning with compression techniques (based on ACA or QR) have been provided in [48]. Given such preconditioning, the extension of subdomains becomes implicit, and multiple-scattering MBFs are simply generated via multiplication to the left by consecutive blocks of the preconditioned system of equations. In [33], it is proven that, if for a given excitation all multiple-scattering MBFs are generated up to order p, then the Krylov subspace of order $q \leq p$ can be constructed with the exclusive help of the MBFs. Mathematically, this reads

$$\mathbf{s}_i^{(q)} = \mathbf{Q}_i^{(p)}\,\mathbf{f}_{p,q} \tag{18}$$

where $\mathbf{s}_i^{(q)}$ is segment i (corresponding to currents in the subdomain i) of generating vector of order $q \leq p$ (i.e., the q-th vector defining the Krylov subpsace, Sec. VI.A); the columns of $\mathbf{Q}_i^{(p)}$ are the MBFs on S_i up to order p; and $\mathbf{f}_{p,q}$ contains coefficients that can be unambiguously determined. Besides the mathematical proof given in [33], an intuitive argument may be advanced to justify the above statement, namely if the generating vectors of the Krylov subspace are created through consecutive left-multiplications by the entire matrix $\boldsymbol{\mathcal{Z}}$, then they can only involve series of "consecutive" blocks of $\boldsymbol{\mathcal{Z}}$,

left-multiplying a segment $\mathbf{w}_i$ of the excitation vector. As a reminder "consecutive" means here that, if block $\mathcal{Z}_{ij}$ left-multiplies block $\mathcal{Z}_{kl}$, then $j = k$. If the preconditioned system of equations is used, the segment $\mathbf{w}_i$ actually corresponds to a primary MBF, while the products that appear in the formation of the generating vectors simply correspond to multiple-scattering MBFs. Hence, the segments of the different generating vectors are linear combinations of MBFs, and as far as the Krylov subspace is considered as a meaningful basis for the entire solution, the above property indicates that the multiple-scattering MBFs are going to form an equally meaningful basis, when used on their respective subdomains. This alleviates the problem with the issue of completeness of the MBF subspace. However, as mentioned above, the number of MBFs generated in this way rapidly becomes prohibitive, so much so that higher-order MBFs or MBFs generated through interaction between very distant subdomains in general need to be discarded. If deemed necessary, they can be replaced by MBFs generated by using a different approach. For instance, it is clear that MBFs generated via distant interactions can be very well represented by MBFs generated using plane waves, such that MBFs of orders larger than two may be created based only on interactions between contiguous subdomains.

Regarding the condition imposed by the MBF approach to obtain the solution of $\mathcal{Z}\,\mathbf{x} = \mathbf{w}$, another link can be established with the FOM Krylov iteration [33], which we have re-formulated in Sec. VI.A. Using the definitions in Section II, we provide here a derivation of that property that is more direct in comparison to that given in [33]. Let us denote by $\mathbf{r}_i^{(p)}$ the i-th segment of the residual vector, obtained from the multiple-scattering approach up to the order p, while all MBFs are retained. By construction, the MBF solution is such that $\mathbf{r}_i^{(p)}$ is orthogonal to the MBFs defined on S_i (see (2) and comment below), i.e., $\mathbf{Q}_i^{(p),H}\,\mathbf{r}_i^{(p)} = 0$. Hence, using (18), we have, for $q \leq p$, $\mathbf{s}_i^{(q),H}\,\mathbf{r}_i^{(p)} = \mathbf{f}_{p,q}^H\,\mathbf{Q}_i^{(p),H}\,\mathbf{r}_i^{(p)} = 0$. The same reasoning can be held for all subdomains S_i, such that:

$$\sum_i \mathbf{s}_i^{(q),H}\,\mathbf{r}_i^{(p)} = \mathbf{s}^{(q),H}\,\mathbf{r}^{(p)} = 0 \tag{19}$$

because each term of the sum is zero, which proves that the entire generating vector $\mathbf{s}^{(q)}$ is orthogonal to the entire residual $\mathbf{r}^{(p)}$. In other words, the MBF approach satisfies the orthogonality conditions that characterize the FOM solution of order q equal to or smaller than the multiple-scattering process p (for the FOM condition, see (15) and its interpretation below.) This however supposes that all multiple-scattering MBFs are kept up to order p, which is not truly practical (see above). Also, the MBF solution of order p satisfies more conditions, at the cost of having to work with a larger system of equations, with more unknowns to be determined than is needed in the FOM approach of same order.

Now let us examine an important question regarding the comparison of performance, in terms of accuracy and computational cost, between Krylov-based iteration and MBF-based solution. In [33], an empirical comparison has been performed on different types of examples (arrays, spheres and aircraft). This comparison is limited to the following conditions: the MBFs are generated in an excitation-specific way and through a truncated multiple-scattering process, only up to order two (with the nearest-neighbor preconditioner the higher orders do not seem to significantly improve the accuracy). Numerical experiments have led to the following (albeit preliminary) conclusion: for equal cost in terms of computation time and memory, the accuracy of both methods is similar when the number of iterations of the FOM approach is equal to the number of MBFs per subdomain. This just appears to be a rule of thumb and needs to be further tested with other examples. We provide below one more example, involving a connected array of bowtie antennas, also studied in [64]. The 5×5 array is shown in Fig. 8. In the preconditioning step, all of the neighboring elements are included in the auxiliary subdomain. Fig. 9 shows the port currents obtained when only the element 1 is excited (top line). The ports do not contain a series impedance; simulations are carried out for a frequency of 10 GHz. It can be seen that the port currents on the other elements are not very low as compared to the one in the excited element, as a result of extremely strong coupling. Thus, this strongly coupled array forms a good test case for numerical methods. On the same plot in log scale, the differences between exact and approximate solutions are shown for the MBF approach, with 9 MBFs per subdomain (corresponding here to one antenna) for the preconditoned system of equations, and the errors obtained for the FOM approach with also 9 iterations. It can be seen that a comparable error level is achieved, with a slight advantage for the MBF approach. Quasi-identical error levels, within 1.7 dB on the average, were obtained with 11 iterations for FOM, instead of 9. This new example supports the rule of thumb referred to above. Further tests are now being carried out in the field of metamaterials.

Given this rule of thumb, one may wonder about the real advantage of using MBFs, as compared to iterative techniques, and we offer at least four. First, it is obviously advantageous to reduce the number of DoFs when, because of the level of geometrical detail, the discretization of the structure needs to be much finer than the usual $\lambda/10$ condition. This is particularly true for antenna applications, where the often complex feeding region needs to be modeled with many elementary basis functions. Second, when appropriate general-purpose MBFs can be found, the efficient solution for multiple right-hand sides offers an important advantage. An example where such MBFs can be easily found is non-periodic arrays of antennas; though more challenging structures involving connected elements may also belong to that category. Third, being non-iterative, the MBF approach is much easier to parallelize. Finally, we also observed for the case of scattering by spheres that the rule of thumb referred to above tends to break down for resonant structures, with an important advantage, in terms of accuracy versus computational resources, in favor of the MBF approach. This seems also to be the case for extremely finely meshed structures, such as those studied in [48].

A further link between Krylov-based methods and the MBF approach may lie in the "restart" procedure [59]. For Krylov-based iterations, this means that the solution at a given point can be considered as the new first guess for the iterative technique. Similarly, the MBF-based solution obtained on a given subdomain can be transformed into just one MBF, while

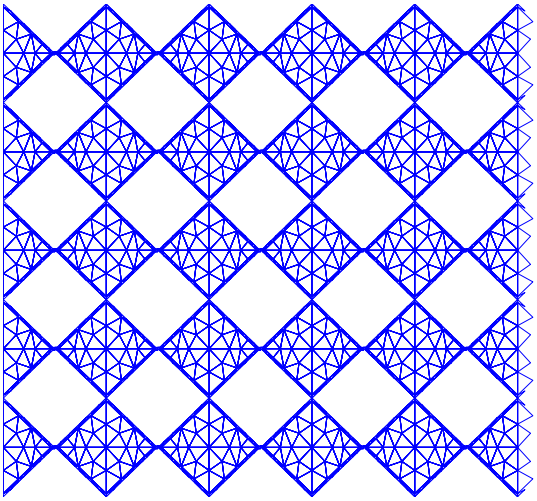

Fig. 8. Mesh used for simulation of 5×5 array of connected bowtie antennas. Element spacing: 1.044 cm horizontally and 1.00 cm vertically.

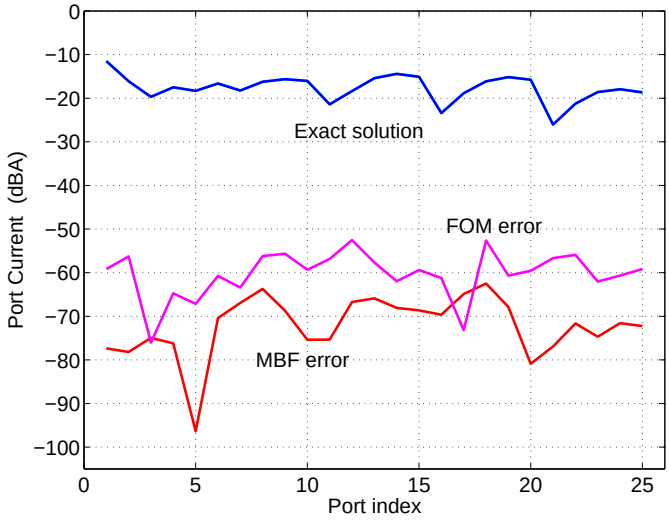

Fig. 9. Exact solution for port currents (numbered left to right, top to bottom, see Fig. 8), and errors obtained with 9 MBFs per subdomain and with 9 FOM iterations.

new MBFs are added, based either on plane-wave excitations or on higher-order multiple scattering. This enables one to refine the solution without augmenting the dimension of the final system of equations. A preliminary study of this approach has been carried out in [64] and may lead to a new direction of research on MBFs and CBFM.

VII. Multi-Scale MBF Analysis

A. Degrees of freedom

Methods relying on MBFs benefit from a reduction in the number of unknowns. This reduction offers a large number of advantages such as the well-known *memory saving* or the use of conventional MoM techniques that have been typically limited in their application to electrically small problems (e.g., [65]). As was previously detailed in Section II, MBFs are defined over a set of contiguous low-level basis functions. In the analysis of antenna arrays, it becomes natural to apply a partitioning so that each subdomain corresponds to an element of the array (e.g., [6]). However, there is nothing that prevents us from defining MBFs for a group of adjacent elements. For the case of electrically large antennas or scatterers, there is no straightforward strategy for the partitioning and the preferred choice is to select the subdomains by grouping basis functions inside certain canonical geometries (e.g., cubes) [38], [66].

At this point, one might wonder how large the *size of the subdomains* should be to define the MBFs. From the solve-time point of view, some criteria have been recently proposed [67] based on minimizing the complexity. However, it does not consider the reduction of the number of unknowns, which is one of the key features of the MBF approach. Although the number of degrees of freedom (DoFs) of radiated and scattered fields is well-known [68], [69], to the best of authors' knowledge, that is not the case when considering the number of DoFs (and so the number of MBFs) for the currents induced on an arbitrary surface.

To further examine this issue, connected with multilevel MBF approaches, we will now present some numerical simulations. Let us first consider a given geometry discretized by means of low-level basis functions, i.e., RWG functions. The object is illuminated by a set of plane waves. As described in Section IV, the current induced by any arbitrary incident field can be calculated as a linear combination of these induced currents. Next, the singular value decomposition is carried out and only those basis functions with a normalized singular value above $\tau = 10^{-4}$ are retained. In other words, this procedure is equivalent to calculating the MBFs for a problem with a single supporting domain so that any potential source of error due to domain extensions is avoided.

In order to choose the number of plane waves, the number of incident angles along θ is set to $N = \lfloor ka \rfloor + 10$, where a is the radius of the minimum sphere enclosing the geometry. It is important to note that this choice, which is similar to the conventional rule for spherical wave truncation [70], fulfills the Nyquist criterion [69]. A similar discretization of the plane wave spectrum is accomplished for each azimuthal circle for a given θ.

The number of surviving MBFs for different spheres and a cylinder is shown in Fig. 10. For the cylinder case, the height is set equal to the radius and no caps are considered (see inset in Fig. 10). In order to check the accuracy of the generated MBFs, the current induced by a linearly polarized plane wave is compared with the current computed using the MoM. For the cylinder case, the plane-wave is assumed to be polarized parallel to the axis of the cylinder and the propagation vector is orthogonal to the aforementioned axis. The error is defined as:

$$e = \frac{\left\| \mathbf{x}^{MBF} - \mathbf{x}^{MoM} \right\|_2}{\left\| \mathbf{x}^{MoM} \right\|_2} \tag{20}$$

where $\mathbf{x}^{MoM}$ and $\mathbf{x}^{MBF}$ are the coefficients of the low-level basis functions using the MoM and the single-block MBF approach. For the sphere case, the error ranges from $5.6 \cdot 10^{-4}$ to $7.7 \cdot 10^{-4}$ whereas this error ranges from $1.3 \cdot 10^{-4}$ to $10 \cdot 10^{-4}$ for the cylinder. This verifies that the generated MBFs are good for modeling an arbitrary induced current.

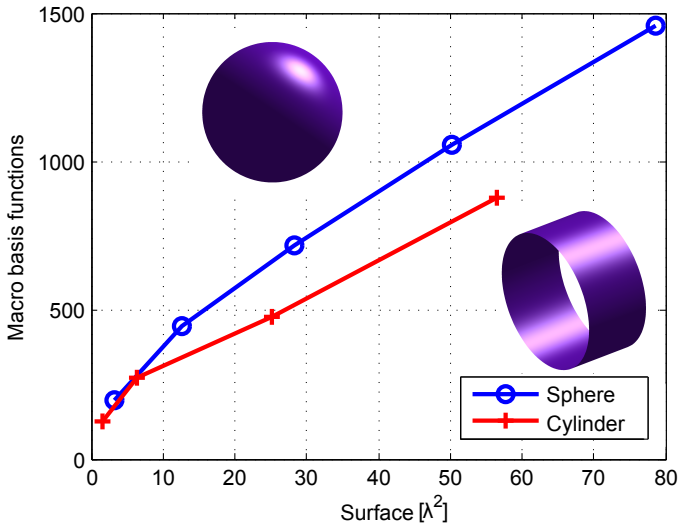

Fig. 10. DoFs for several canonical geometries.

The results presented in Fig. 10 reveal that the asymptotic behavior for large domains is approximately linear. It is interesting to note that the discretization of a geometry with low-level basis functions also involved a linear increase in the number of unknowns versus the surface to be analyzed. However, the slopes of the plots with MBFs are considerably smaller than when we consider low-level basis functions whose proportion is on the order of 100 basis functions per square wavelength. For instance, a sphere with a radius of 2λ (i.e., surface $50.27\lambda^2$) can be modeled with 1056 MBFs whereas the number of low-level basis functions required would be on the order of 5027.

Another interesting fact inferred from Fig. 10 pertains to the number of MBFs needed for electrically small domains. In this case, the asymptotic behavior is not reached and the number of MBFs grows much faster than in the case of electrically larger surfaces. In order to illustrate the validity of the latter observation, let us consider the sphere geometry once again. Furthermore, the relationship between the number of MBFs and domain surface for any arbitrary surface is considered to be equal to that for the sphere. This assumption is reasonable since the behavior of the curves in Fig. 10 has also been observed for other geometries such as plates or cubes. Under the previous hypotheses, an MBF method working with domains of $28.9\lambda^2$ will require approximately 2.47 times fewer unknowns than needed using the same MBFs method working with domains of $3.2\lambda^2$. However, increasing the size of the domain surface requires the handling of much larger blocks and, consequently, the computationally burden is significantly increased in this case. In the next section, techniques to mitigate this computational burden are described.

Finally, it is worthwhile to remark that similar observations have also been made by a number of different authors. For example, this fact was observed in [71] and exploited to generate MBFs on large blocks by applying physical optics. Similarly, the analysis of some particular geometries for different block sizes revealed that fewer MBFs are required when employing larger blocks to achieve the same prescribed error level [33].

B. Multilevel MBF approach

The aforementioned behavior of the DoFs versus the domain size suggests that the best compression rates are achieved for electrically large subdomains. Nevertheless, generating MBFs for these subdomains can be computationally expensive. Moreover, the generation becomes more demanding when applying the plane wave spectrum approach since the currents on each subdomain has to be solved for multiple right hand sides. In order to benefit from the reduction in number of unknowns, while maintaining the computational burden at a reasonable level, a multilevel scheme which is referred to as *Multilevel Characteristic Basis Function Method* (MLCBFM) [21], [22] has been proposed. This technique is based on a recursive generation of the macrobasis functions. A hierarchical partitioning of the geometry is required before applying the multilevel approach. This step is illustrated in Fig. 11 for the NASA almond in the context of a two-level scheme. In this figure, a gap has been introduced between geometry partitions to emphasize the domains. Next, the macrobasis functions are generated from the bottom to the top level. At each level, the basis functions are expressed as linear combinations of the basis functions defined on the level underneath. Let us consider a multilevel MBF at the l-th level, which is denoted by $\mathcal{F}^{(l)}$. The number of subdomains of level $l-1$ inside the domain is given by N while the number of MBFs for the n subdomain is given by $C(n)$. Then, according to the multilevel definition of the MBFs, $\mathcal{F}^{(l)}$ can be expressed as:

$$\mathcal{F}^{(l)} = \sum_{n=1}^{N} \sum_{i=1}^{C(n)} q_{ni}^{(l-1)} \mathcal{F}_{ni}^{(l-1)} \tag{21}$$

where $q_{nj}^{(l-1)}$ are the weights of the linear combinations that are computed in the process of generation of the MBFs.

Once the coefficients of the MBFs have been computed at each level, the matrix of the system of equations and the right hand side can be recursively computed from bottom to top by carrying out pre- and post-multiplications by the coefficients of the matrices containing the coefficients of the MBFs at the corresponding level.

The above formulation can be applied to an *arbitrary number of levels* to benefit from the compression rate associated with large blocks. Nevertheless, the number of MBFs for very large blocks, which is assumed to be independent of the number of underlying levels, prevents us from handling extremely large blocks. In other words, as long as the MBFs are correctly generated at each level, the number of DoFs at the top level is expected to depend only on the domain extension. Consequently, very large domain extensions involve a large number of DoFs and, therefore, upper levels cannot be efficiently handled because the number of underlying MBFs becomes very large.

Our experience is that a *two-level scheme* provides a good trade-off between accuracy and compression rate without significantly increasing the computational burden. There appears to be a consensus among other authors [21], [22], [72], [73] on this issue, since they also limited the implementation to two levels.

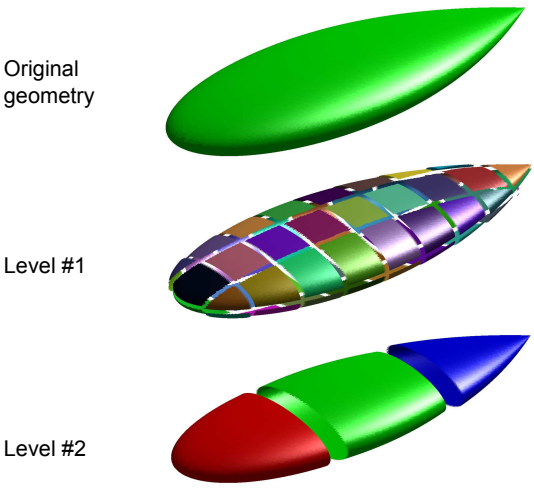

Fig. 11. Multilevel partitioning of the NASA almond.

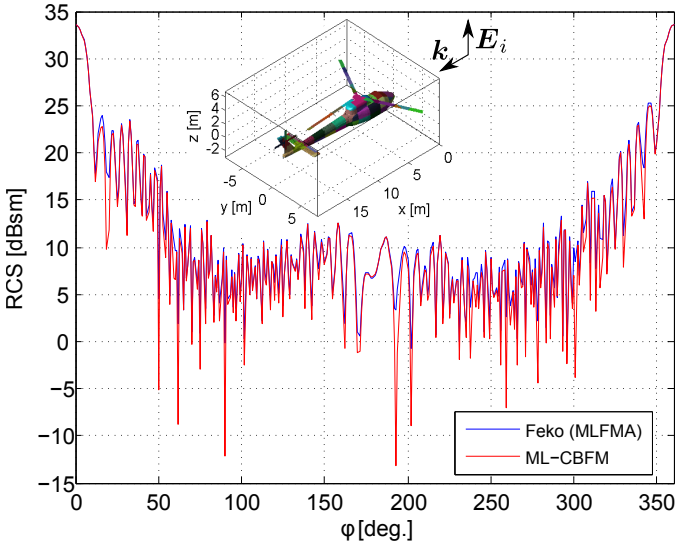

Fig. 12. Bistatic RCS for the helicopter. The inset shows the first level partitioning.

In order to illustrate the multilevel approach, the bistatic radar cross section (RCS) of a *helicopter-type geometry* is considered. The problem is discretized at 400 MHz by using 96844 RWG basis functions. Next, the surface is partitioned so that the low-level basis functions are grouped into 420 domains for the first-level (i.e., conventional) MBFs (see Fig. 12). Generating the corresponding MBFs by using the plane-wave spectrum approach, followed by an SVD thresholding with $\tau = 10^{-4}$, results in a problem with 13275 unknowns. Next, these first-level MBFs are grouped into three second-level domains which corresponds to splitting the geometry into three blocks along the x-axis. As a consequence, the final number of unknowns (i.e., second-level MBFs) is reduced to only 3192.

The *bistatic radar cross section* for the case of an incident field $\boldsymbol{E}_i = \exp(j\,k\,x)\,\hat{z}$ is shown in Fig. 12. The results obtained using the MLFMA implemented in the commercial software FEKO [74] are also shown for comparison purposes. The agreement between the two methods is seen to be excellent.

VIII. Conclusions and Outlook

Integral-equation approaches remain among the most competitive methods for the solution of large radiation or scattering problems. Domain decomposition started to be applied to this type of methods about fifteen years ago and has been introduced at about the same time by different labs, in several variants. They rely on the *a priori* determination of the subspace in which current distributions (or equivalent currents) on a given subdomain can be found. Those subspaces are subtended by Macro Basis Functions (MBFs), defined in terms of the original elementary basis functions. Their main advantage is that they allow the direct solution of large problems, thereby avoiding the uncertainty about the number of iterations and enabling very quick solutions for multiple excitations. We reviewed different techniques for the determination of the MBFs, as well as methods for the very fast calculation of their reactions. We also reviewed the similarities between this class of methods and Krylov-based iterative techniques, like the Full Orthogonalization Method (FOM). Besides the direct-solution aspect, the domain-decomposition nature of MBF-based methods allows one to enforce boundary-type conditions on each subdomain individually.

This type of methods is particularly well-suited for application to geometries for which the characteristic dimensions of the mesh are very much finer than the wavelength, such that the number of physical degrees of freedom of the fields is much smaller than those implied by the complexity of the geometrical discretization. Such geometries are extremely common in industrial applications. MBFs can be applied to preconditioned systems of equations, which can implicitly account for the connectivity between subdomains without significant loss of accuracy. Besides, beyond this preconditioning, the MBF approach in itself seems to add its own preconditioning effect, such that practically no loss of accuracy is observed when solving scattering problems on objects near resonance. Being non-iterative in nature, the MBF approach lends itself very well to parallelization, which means that the MBF methodology is among the approaches that will at best benefit from the current strong trend toward large-scale multiple-core calculation.

It is expected that improved construction of MBFs, faster interaction methods and multi-level approaches will receive more attention in the coming years. As previously pointed out, the generation of MBFs yields a different number of unknowns, depending on the employed scheme. Problems requiring a restricted set of excitations can benefit from the high compression provided by the primary-secondary approach (or its extension to higher orders) without a significant loss of accuracy. On the other side, the plane-wave approach enables us to compute excitation-free MBFs at the cost of an increment in the number of degrees of freedom. This fact suggests that *a priori* knowledge of the excitation can be employed to decrease the degrees of freedom in the problem.

Moreover, considering larger domains in the MBF generation seems to (proportionally) require fewer unknowns, setting

the basis for the multilevel formulation. This probably results from the fact that more information is used during the MBFs generation and, consequently, the achieved MBFs can better model the final currents. Thus, a rigorous study is still needed regarding the minimum number of degrees of freedom to be associated with a given problem, and regarding how to fully exploit all the *a priori* information about optimum domain size and excitation. Regarding the latter, for instance, excitation-dependent MBFs may remain valid when the primary source is moved over a finite domain. MBFs may also have a regularizing effect in the solution of radiation or scatering problems. Besides providing more stable solutions, their physics-based foundation can also serve purposes that are other than purely computational. For instance, they have been exploited for calibration purposes in [75]–[78]. They could also be exploited with advantage in time-domain solution schemes, since MBF-type basis functions in the time domain have been observed to provide a better late-time stability [79].

To conclude, MBF methods and related techniques have already proved quite powerful for the solution of Maxwell's equations in surface integral-equation form. Over the past decade, they have been strongly accelerated and methodologies to produce more complete sets of MBFs have been developed. Their direct-solution nature and their ease of parallelization make them preferable to iterative techniques for a wide class of problems. Nevertheless, it is expected that combined research on MBF-based and iterative techniques will be beneficial to the development of both solution methodologies. Further progress in this area may also benefit from continued research on the physical degrees of freedom of fields excited on arbitrarily-shaped structures, with possible applications beyond those in computational methods.

ACKNOWLEDGEMENT

The authors thank Shambhu Nath Jha for his help with the production of Fig. 7.

REFERENCES

[1] R. Mittra, "A look at some challenging problems in computational electromagnetics," *IEEE Antennas Propag. Mag.*, vol. 46, no. 5, pp. 18–32, May 2004.

[2] G. A. E. Vandenbosch and A. R. Van de Cappelle, "Use of combined expansion scheme to analyze microstrip antennas with the method of moments," *Radio Sci.*, vol. 27, no. 6, pp. 911–916, Dec. 1992.

[3] J. Heinstadt, "New approximation technique for current distribution in microstrip array antennas," *Micr. Opt. Technol.*, vol. 29, pp. 1809–1810, Oct. 1993.

[4] S. Ooms and D. De Zutter, "A new iterative diakoptics-based multilevel moments method for planar circuits," *IEEE Trans. Microw. Theory Tech.*, vol. 46, no. 3, pp. 280–291, mar. 1998.

[5] E. Suter and J. R. Mosig, "A subdomain multilevel approach for the efficient MoM analysis of large planar antennas," *Micr. Opt. Technol.*, vol. 26, no. 4, pp. 270–277, Aug. 2000.

[6] V. Prakash and R. Mittra, "Characteristic basis function method: A new technique for efficient solution of method of moments matrix equations," *Micr. Opt. Technol.*, vol. 36, pp. 95–100, Jan. 2003.

[7] L. Matekovits, G. Vecchi, G. Dassano, and M. Orefice, "Synthetic function analysis of large printed structures: the solution space sampling approach," in *Proc. IEEE AP-S International Symposium*, Boston, Massachusetts, July 2001, pp. 568–571.

[8] G. Tiberi, A. Monorchio, G. Manara, and R. Mittra, "Hybridizing asymptotic and numerically rigorous techniques for solving electromagnetic scattering problems using the characterisitic basis functions (CBFs)," in *Proc. IEEE AP-S International Symposium*, Columbus, Ohio, June 2003, pp. 22–27.

[9] J. Yeo, V. Prakash, and R. Mittra, "Efficient analysis of a class of microstrip antennas using the Characteristic Basis Function Method (CBFM)," *Micr. Opt. Technol.*, vol. 39, pp. 456–464, Dec. 2003.

[10] J. Laviada, M. R. Pino, and F. Las-Heras, "Generation of excitation-independent characteristic basis functions for three-dimensional homogeneous dielectric bodies," *IEEE Trans. Antennas Propag.*, vol. 59, no. 9, pp. 3318–3327, Sept. 2011.

[11] S. J. Kwon, K. Du, and R. Mittra, "Characteristic basis function method: A numerically efficient technique for analyzing microwave and rf circuits," *Micr. Opt. Technol.*, vol. 38, no. 6, pp. 444–448, July 2003.

[12] R. Maaskant, P. Takook, and P.-S. Kildal, "Fast analysis of gap waveguides using the characteristic basis function method and the parallel-plate Green's function," in *Proc. Int. Conf. on Electromagn. in Adv. Applicat. (ICEAA)*, CapeTown, South Africa, Sept. 2012, pp. 788–791.

[13] R. Mittra, G. Bianconi, C. Pelletti, K. Du, S. Genovesi, and A. Monorchio, "Fast-factorization acceleration of MoM compressive domain-decomposition," *Proc. of the IEEE*, vol. 100, no. 7, pp. 2122–2131, jul. 2011.

[14] C. Delgado, M. F. Catedra, and R. Mittra, "Efficient multilevel approach for the generation of characteristic basis functions for large scatters," *IEEE Trans. Antennas Propag.*, vol. 56, no. 7, pp. 2134–2137, July 2008.

[15] R. Maaskant, M. V. Ivashina, O. Iupikov, E. A. Redkina, S. Kasturi, and D. H. Schaubert, "Analysis of large microstrip-fed tapered slot antenna arrays by combining electrodynamic and quasi-static field models," *IEEE Trans. Antennas Propag.*, vol. 56, no. 6, pp. 1798–1807, June 2011.

[16] R. Maaskant, R. Mittra, and A. G. Tijhuis, "Application of trapezoidal-shaped characteristic basis functions to arrays of electrically interconnected antenna elements," in *Proc. Int. Conf. on Electromagn. in Adv. Applicat. (ICEAA)*, Torino, Sept. 2007, pp. 567–571.

[17] J. Laviada, M. R. Pino, F. Las-Heras, and R. Mittra, "Interpolation scheme for fast calculation of reaction terms in the characteristic basis function method," *Micr. Opt. Technol.*, vol. 51, no. 8, pp. 1818–1824, Aug. 2009.

[18] E. Garcia, C. Delgado, I. Diego, and M. Catedra, "An iterative solution for electrically large problems combining the characteristic basis function method and the multilevel fast multipole algorithm," *IEEE Trans. Antennas Propag.*, vol. 56, no. 8, pp. 2363–2371, Aug. 2008.

[19] E. Garcia, C. Delgado, I. Gonzalez, and F. Cátedra, "Efficient parallelization of a CBFM-MLFMA scheme for the computation of complex electromagnetic problems," in *Proc. IEEE AP-S International Symposium*, San Diego, California, July 2008, pp. 1–4.

[20] D. J. Ludick and D. B. Davidson, "Investigating efficient parallelization techniques for the characteristic basis function method (CBFM)," in *Proc. Int. Conf. on Electromagn. in Adv. Applicat. (ICEAA)*, Torino, Sept. 2009, pp. 400–403.

[21] J. Laviada, F. Las-Heras, M. R. Pino, and R. Mittra, "Solution of electrically large problems with multilevel characteristic basis functions," *IEEE Trans. Antennas Propag.*, vol. 57, no. 10, pp. 3189–3198, Oct. 2009.

[22] R. Maaskant, R. Mittra, and A. G. Tijhuis, "Multi-level characteristic basis function method (CBFM) for the analysis of large antenna arrays," *Special Issue on: CEM for Modeling Large Finite Antenna Arrays, The Radio Science Bullentin*, vol. 336, no. 3, pp. 23–34, 2011.

[23] L. Matekovits, G. Vecchi, and V. A. Laza, "Degrees of freedom and synthetic functions in the analysis of large antennas," in *International URSI Commission B - Electromagnetic Theory Symposium, EMTS*, Pisa, Italy, May 2004, pp. 138–140.

[24] L. Matekovits, V. A. Laza, and G. Vecchi, "Analysis of large complex structures with the synthetic-functions approach," *IEEE Trans. Antennas Propag.*, vol. 55, no. 9, pp. 2509–2521, Sept. 2007.

[25] P. D. Vita, A. Freni, L. Matekovits, P. Pirinoli, and G. Vecchi, "A combined AIM-SFX approach for large complex arrays," in *Proc. IEEE AP-S International Symposium*, Honulollu, Hawaii, June 2007, pp. 3452–3455.

[26] L. Matekovits, G. Vecchi, M. Bercigli, and M. Bandinelli, "Synthetic-functions analysis of large aperture-coupled antennas," *IEEE Trans. Antennas Propag.*, vol. 57, no. 7, pp. 1936–1943, July 2009.

[27] P. Pirinoli, L. Matekovits, F. Vipiana, G. Vecchi, and M. Orefice, "Multi-grid SFX-MR approach for the analysis of large arrays," in *18th International Conference on Applied Electromagnetics and Communications (ICECom)*, Dubrovnik, Croatia, Oct. 2005, pp. 1–4.

[28] C. Craeye, "Finite-array characterization with the help of the ASM-MBF method : Eigenmode analysis," in *International URSI Commission B - Electromagnetic Theory Symposium, EMTS*, Berlin, Germany, Aug. 2010, pp. 168–170.

[29] ——, "A fast impedance and pattern computation scheme for finite antenna arrays," *IEEE Trans. Antennas Propag.*, vol. 54, no. 10, pp. 3030–3034, Oct. 2006.

[30] S. N. Jha and C. Craeye, "Fast spectral-domain MBF method for printed antennas," in *Proc. European Conference on Antennas and Propag. (EuCAP)*, Prague, Slovakia, Mar. 2012, pp. 292–295.

[31] D. Gonzalez-Ovejero, E. Acedo, N. Razavi-Ghods, and C. Craeye, "Fast MBF based method for large random array characterization," in *Proc. IEEE AP-S International Symposium*, Charleston, South Carolina, June 2009, pp. 1522–3965.

[32] C. Craeye, "On the connection between multiple-scattering based macro basis functions and Krylov subspace methods," in *Proc. Int. Conf. on Electromagn. in Adv. Applicat. (ICEAA)*, Torino, Sept. 2009, pp. 938–941.

[33] N. A. Ozdemir, D. Gonzalez-Ovejero, and C. Craeye, "On the relationship between multiple-scattering macro basis functions and Krylov subspace iterative methods," *IEEE Trans. Antennas Propag.*, vol. 61, no. 4, pp. 2088–2098, Apr. 2013.

[34] W. B. Lu, T. J. Cui, Z. G. Qian, X. X. Yin, and W. Hong, "Accurate analysis of large-scale periodic structures using an efficient sub-entire-domain basis function method," *IEEE Trans. Antennas Propag.*, vol. 52, no. 11, pp. 3078–3085, Nov. 2004.

[35] D. J. Bekers, S. J. L. van Eijndhoven, A. A. F. van de Ven, P. P. Borsboom, and A. G. Tijhuis, "Eigencurrent analysis of resonant behavior in finite antenna arrays," *IEEE Trans. Microw. Theory Tech.*, vol. 54, no. 6, pp. 2821–2829, June 2006.

[36] V. Lancellotti, B. P. de Hon, and A. G. Tijhuis, "An eigencurrent approach to the analysis of electrically large 3-D structures using linear embedding via Green's operators," *IEEE Trans. Antennas Propag.*, vol. 57, no. 11, pp. 3575–3585, Nov. 2009.

[37] S. M. Rao, "A true domain decomposition procedure based on method of moments to handle electrically large bodies," *IEEE Trans. Antennas Propag.*, vol. 60, no. 9, pp. 4233–4238, Sept. 2012.

[38] E. Lucente, A. Monorchio, and R. Mittra, "An iteration-free MoM approach based on excitation independent characteristic basis functions for solving large multiscale electromagnetic scattering problems," *IEEE Trans. Antennas Propag.*, vol. 56, no. 4, pp. 999–1007, Apr. 2008.

[39] L. Crocco, F. Cuomo, and T. Isernia, "Generalized scattering-matrix method for the analysis of two-dimensional photonic bandgap devices," *J. Opt. Soc. Am. A*, vol. 24, no. 10, pp. A12–A22, Oct 2007.

[40] R. F. Harrington, *Time-Harmonic Electromagnetic Fields*. New York and London: McGraw-Hill Book Company, 1961.

[41] S. G. Hay and J. D. O'Sullivan, "Analysis of common-mode effects in a dual-polarized planar connected-array antenna," *Radio. Sci.*, vol. 43, 2008.

[42] C. Craeye, T. Gilles, and X. Dardenne, "Efficient full-wave characterization of arrays of antennas embedded in finite dielectric volumes," *Radio. Sci.*, vol. 44, 2009.

[43] G. Bianconi, C. Pelletti, and R. Mittra, "A high-order characteristic basis function algorithm for an efficient analysis of printed microwave circuits and antennas etched on layered media," *IEEE Antennas Wireless Propag. Lett.*, vol. 12, pp. 543–546, 2013.

[44] D. Pissoort, E. Michielssen, D. V. Ginste, and F. Olyslager, "A rank-revealing preconditioner for the fast integral-equation based characterization of electromagnetic crystal devices," *Microw. Opt. Technol. Lett.*, vol. 48, no. 4, pp. 783–789, Apr. 2006.

[45] C. Craeye and R. Sarkis, "Finite array analysis through combination of Macro Basis Functions and Array Scanning Methods," *Journal of Applied Comput. Electromagnetics Soc. (ACES)*, vol. 23, no. 3, pp. 255–261, Sept. 2008.

[46] B. Munk and G. Burrell, "Plane-wave expansion for arrays of arbitrarily oriented piecewise linear elements and its application in determining the impedance of a single linear antenna in a lossy half-space," *IEEE Trans. Antennas Propag.*, vol. 27, no. 3, pp. 331–343, may. 1979.

[47] C. Craeye, B. Andrés-García, E. García-Munoz, and R. Sarkis, "An Open-Source Code for the Calculation of the Effects of Mutual Coupling in Arrays of Wires and for the ASM-MBF Method," *International Journal of Antennas and Propagation*, vol. 2010, no. Article ID 137903, p. 10, 2010.

[48] N. Ozdemir, D. Gonzalez-Ovejero, and C. Craeye, "A near-field preconditioner preserving the low-rank representation of Method of Moments interaction matrices," in *Proc. ICEAA conf.*, Torino, Sept.9–12 2013.

[49] M. Bebendorf, "Approximation of boundary element matrices," *Numer. Math.*, vol. 86, no. 4, pp. 565–589, June 2000.

[50] K. Zhao, M. N. Vouvakis, and J. F. Lee, "The adaptive cross approximation algorithm for accelerated method of moments computations of EMC problems," *IEEE Trans. Electromagn. Compat.*, vol. 47, no. 4, pp. 763–773, Nov. 2005.

[51] N. Ozdemir and J.-F. Lee, "A low-rank IE-QR algorithm for matrix compression in volume integral equations," *IEEE Trans. Magn.*, vol. 40, no. 2, pp. 1017–1020, mar. 2004.

[52] O. Bucci, C. Gennarelli, and C. Savarese, "Representation of electromagnetic fields over arbitrary surfaces by a finite and nonredundant number of samples," *IEEE Trans. Antennas Propag.*, vol. 46, no. 3, pp. 351–359, Mar. 1998.

[53] D. Gonzalez-Ovejero and C. Craeye, "Interpolatory macro basis functions analysis of non-periodic arrays," *IEEE Trans. Antennas Propag.*, vol. 59, no. 8, pp. 3117–3122, Aug 2011.

[54] ——, "Accelerated macro basis functions analysis of finite printed antenna arrays through 2d and 3d multipole expansions," *IEEE Trans. Antennas Propag.*, vol. 61, no. 2, pp. 707–717, Feb 2012.

[55] R. Boix, F. Mesa, and F. Medina, "Application of total least squares to the derivation of closed-form greens functions for planar layered media,," *IEEE Trans. Antennas Propag.*, vol. 55, no. 2, pp. 268–280, Feb. 2007.

[56] G. Tiberi, A. Monorchio, G. Manara, and R. Mittra, "A spectral domain ie method utilizing analytically derived characteristic basis functions for the scattering from large faceted objects," *IEEE Trans. Antennas Propag.*, vol. 54, no. 9, pp. 2508–2514, Sep 2006.

[57] A. Freni, P. De Vita, P. Pirinoli, L. Matekovits, and G. Vecchi, "Fast-factorization acceleration of MoM compressive domain-decomposition," *IEEE Trans. Antennas Propag.*, vol. 59, no. 12, pp. 4588–4599, dec. 2011.

[58] A. Greenbaum, "Iterative Methods for Solving Linear Systems," in *Frontiers in Applied Mathematics*. SIAM, 1997, vol. 17.

[59] Y. Saad and M. H. Schultz, "GMRES: A Generalized Minimal Residual Algorithm for Solving Nonsymmetric Linear Systems," *SIAM Journal on Scientific and Statistical Computing*, vol. 7, no. 3, pp. 856–869, 1986.

[60] K. Cools, F. Andriulli, and E. Michielssen, "A calderón multiplicative preconditioner for the pmchwt integral equation," *IEEE Trans. Antennas Propag.*, vol. 59, no. 12, pp. 4579–4587, Dec. 2011.

[61] H. A. van der Vorst, "Krylov subspace iteration," *Computing in Science and Engineering*, vol. 2, no. 1, pp. 32–37, 2000.

[62] R. Maaskant, R. Mittra, and A. G. Tijhuis, "Fast analysis of large antenna arrays using the characteristic basis function method and the adaptive cross approximation algorithm," *IEEE Trans. Antennas Propag.*, vol. 56, no. 11, pp. 3440–3451, Nov. 2008.

[63] E. Lucente, A. Monorchio, and R. Mittra, "An iteration-free MoM approach based on excitation independent characteristic basis functions for solving large multiscale electromagnetic scattering problems," *IEEE Trans. Antennas Propag.*, vol. 56, no. 4, pp. 999–1007, Apr. 2008.

[64] C. Craeye, "Further comparison between Macro Basis Functions and Krylov subspace iterative methods," in *Proc. of PIERS Conference*, Xian, Mar. 22–26, 2010.

[65] J. Laviada, J. Gutierrez-Meana, M. R. Pino, and F. Las-Heras, "Analysis of partial modifications on electrically large bodies via characteristic basis functions," *IEEE Antennas Wireless Propag. Lett.*, vol. 9, no. 1, pp. 834–837, 2010.

[66] C. Delgado, M. Catedra, and R. Mittra, "Application of the characteristic basis function method utilizing a class of basis and testing functions defined on nurbs patches," *IEEE Trans. Antennas Propag.*, vol. 56, no. 3, pp. 784–791, Mar. 2008.

[67] K. Konno, C. Qiang, K. Sawaya, and T. Sezai, "Optimization of block size for CBFM in MoM," *IEEE Trans. Antennas Propag.*, vol. 60, no. 10, pp. 4719–4724, Oct. 2012.

[68] A. Yaghjian, "An overview of near-field antenna measurements," *IEEE Trans. Antennas Propag.*, vol. 34, no. 1, pp. 30–45, Jan. 1986.

[69] O. Bucci and G. Franceschetti, "On the degrees of freedom of scattered fields," *IEEE Trans. Antennas Propag.*, vol. 37, no. 7, pp. 918–926, July 1989.

[70] J. E. Hansen, *Spherical near-field antenna measurements*. London, UK: Peter Peregrinus Ltd, 1988.

[71] C. Delgado, F. Cátedra, and R. Mittra, "A numerically efficient technique for orthogonalizing the basis functions arising in the solution of electromagnetic scattering problems using the CBFM," in *Proc. IEEE AP-S International Symposium*, Honululu, Hawaii, June 2007, pp. 3608–3611.

[72] J. Hu, W. Lu, H. Shao, and Z. Nie, "Electromagnetic analysis of large scale periodic arrays using a two-level CBFs method accelerated with FMM-FFT," *IEEE Trans. Antennas Propag.*, vol. 60, no. 12, pp. 5709–5716, Dec. 2012.

[73] X. Chen, C. Gu, J. Ding, Z. Li, and Z. Niu, "Direct solution of electromagnetic scattering from perfect electric conducting targets using multilevel characteristic basis function method with adaptive cross

approximation algorithm," *IET Microwaves, Antennas & Propagation*, vol. 7, no. 3, pp. 195–201, Feb. 2013.
[74] (2012) EM Software & Systems – S.A. (Pty) Ltd, Stellenbosch, South Africa, FEKO, Suite 6.2. [Online]. Available: http://www.feko.info
[75] G. Hislop, S. Lambot, D. Gonzalez-Ovejero, and C. Craeye, "Antenna calibration for near-field problems with the Method of Moments," in *Proc. EUCAP conf.*, Rome, Apr. 2011.
[76] R. Maaskant, M. Ivashina, S. Wijnholds, and K. F. Warnick, "Efficient prediction of array element patterns using physics-based expansions and a single far-field measurement," *IEEE Trans. Antennas Propag.*, vol. 60, no. 8, pp. 3614–3621, Aug 2012.
[77] A. Young, R. Maaskant, M. Ivashina, D. I. L. de Villiers, and D. Davidson, "Accurate beam prediction through characteristic basis function patterns for the MeerKAT/SKA radio telescope antenna," *IEEE Trans. Antennas Propag.*, vol. 61, no. 5, pp. 2466–2473, May 2013.
[78] E. de Lera Acedo, C. Craeye, N. Razavi-Ghods, and Gonzalez-Ovejero, "Low order beam models for the calibration of large aperture arrays for radio astronomy: the case of the SKA-low instrument,," in *Proc. ICEAA conf.*, Torino, Sept.9–12 2013.
[79] T. Sarkar, W. Lee, and S. Rao, "Analysis of transient scattering from composite arbitrarily shaped complex structures," *IEEE Trans. Antennas Propag.*, vol. 48, 2000.

Christophe Craeye received the Electrical Engineer and Bachelor in Philosophy degrees in 1994, from the Université catholique de Louvain (UCL). In 1998 received the Ph.D. degree from UCL, in the field of scattering by the sea surface (collaboration with NASA and ESA). From 1999 to 2001, he stayed as a post-doc researcher at the Eindhoven University of Technology, where he worked on the Square Kilometer Array radio telescope project. In this framework, he also stayed at the University of Massachusetts in the Fall of 1999, and worked with the Netherlands Institute for Research in Astronomy in 2001. In 2002 he started an antenna research activity at UCL, where he is now a Professor. He stayed at the University of Cambridge (Astrophysics and Detectors group) from January to August 2011. His research interests are finite antenna arrays, wideband antennas, small antennas, metamaterials and numerical methods for fields in periodic media, with applications to communication and sensing . He served as an Associate Editor of the IEEE Transactions on Antennas and Propagation from 2004 to 2010, he is now an Associate Editor for IEEE Antennas and Wireless Propagation Letters. In 2009, he received the 2005-2008 Georges Vanderlinden prize from the Belgian Royal Academy of Sciences

Jaime Laviada was born in Gijn, Spain. He received the M.S. degree in telecommunication engineering and the Ph.D. degree from the University of Oviedo, Gijón, Spain, in 2005 and 2010, respectively.

In 2006, he joined the research group Signal Theory and Communications, Department of Electrical Engineering, University of Oviedo. He was a Visiting Scholar in the Electromagnetics and Communications Lab, Pennsylvania State University, State College, PA, USA, during 2007 and 2008.

He has been involved in multiple national and European projects as well as multinational company contracts. His main research interests are in numerical efficient techniques applied to antenna measurements, method of moments, and antenna pattern synthesis.

Rob Maaskant received his M.Sc. degree (*cum laude*) in 2003, and his Ph.D. degree (*cum laude*) in 2010, both in Electrical Engineering from the Eindhoven University of Technology, Eindhoven, The Netherlands. His Ph.D. has been awarded "the best dissertation of the Electrical Engineering Department, 2010." From 2003–2010, he was employed as an antenna research scientist at the Netherlands Institute for Radio Astronomy (ASTRON), Dwingeloo, The Netherlands, and from 2010–2012 as a postdoctoral researcher in the Antenna Group of the Signals and Systems Department at the Chalmers University of Technology, Sweden, for which he won a European Commission FP7 Marie Sklodowska-Curie Actions Outgoing – Rubicon Fellowship from the Netherlands Organization for Scientific Research (NWO), 2010. He is currently an Assistant Professor in the same Antenna Group. He is the primary author of the CAESAR software; an advanced integral-equation based solver for the analysis of large antenna array systems. His current research interest is in the field of receiving antennas for low-noise applications, meta-material based waveguides, and computational electromagnetics to solve these types of problems.

Dr. Maaskant received the 2nd best paper prize ('best team contribution') at the 2008 ESA/ESTEC workshop, Noordwijk, and was awarded a Young Researcher grant from the Swedish Research Council (VR), in 2011. He is an Associate Editor of both the IEEE Transactions on Antennas and Propagation and the FERMAT journal.

Raj Mittra is a Professor in the Electrical Engineering department of the Pennsylvania State University, where he is the Director of the Electromagnetic Communication Laboratory. Prior to joining Penn State he was a Professor in the Electrical and Computer Engineering at the University of Illinois in Urbana Champaign from 1957 through 1996, when he moved to his present position at the Penn State University.

He is a Life Fellow of the IEEE, a Past-President of AP-S, and he has served as the Editor of the Transactions of the Antennas and Propagation Society. He won the Guggenheim Fellowship Award in 1965, the IEEE Centennial Medal in 1984, and the IEEE Millennium medal in 2000. Other honors include the IEEE/AP-S Distinguished Achievement Award in 2002, the Chen-To Tai Education Award in 2004 and the IEEE Electromagnetics Award in 2006, and the IEEE James H. Mulligan Award in 2011.